CdTe sensor configurations for robot assisted photon counting gamma camera

J. Fey, S. Procz, M.K. Schütz, Vincent Schoepff, Frederick Carrel, J.S. Useche, A. Fauler, M. Fiederle

Article

CdTe sensor configurations for Robot assisted photon counting gamma camera

Julian Fey[1], Simon Procz[1], Michael K. Schütz[1], Vincent Schoepff[2], Frédérick Carrel[2], Juan S. Useche[1], Alex Fauler[1] and Michael Fiederle[1]

[1] Freiburg Materials Research Center, Albert-Ludwigs-Universität Freiburg, D-79104 Freiburg, Germany; julian.fey@fmf.uni-freiburg.de
[2] CEA, List, F-91191 GIF-SUR-YVETTE Cedex, France; vincent.schoepff@cea.fr
* Correspondence: julian.fey@fmf.uni-freiburg.de

Received: date; Accepted: date; Published: date

Abstract: In this work, different Cadmium Telluride (CdTe) sensor configurations are assessed for the usage in a robot assisted portable gamma camera. In the first part, four CdTe sensors, with thickness of 0.45 mm, 1 mm, 2 mm and 3 mm and pixel sizes of 55 μm and 110 μm, are investigated regarding their spectroscopic performance. The photon counting detector Timepix1 is hereby used. The 3 mm CdTe sensor shows increase in count rate up to a factor of 1.25 compared to a 2 mm CdTe sensor, 1.84 compared to a 1 mm CdTe sensor and up to 2.71 compared to a 0.45 mm CdTe sensor in the case of ^{137}Cs. In the second part, the 3 mm CdTe sensor was implemented in a commercially available gamma camera, the iPIX. The system was integrated in the bomb disposal robot and tested in different scenarios. The integrated 3 mm CdTe detector measured 21.5 counts per second emitting from a ^{60}Co source with an activity of 2.8 ± 0.07 Gbq in 20-meters distance in an open environment. The acquisition time was 116 seconds. The angular resolution was sufficient for the user to localize the radioactive isotope inside the test structure.

Keywords: CdTe; Photon counting; Timepix; Gamma camera; Spectroscopy.

1. Introduction

The threat to public safety posed by improvised explosive devices (IEDs) has increased significantly in recent years [1]. In the context of IED, one of the most important aspects, both in terms of real danger and media presence, is the threat of radiological dispersal devices (RDDs). The primary goal of RDDs is neither the damaging of infrastructure nor the injuring of people by the explosive effect, but rather, the contamination of the largest possible area by radioactive substances. The current development state of semiconductor sensors for the detection of both, hard X-ray and gamma-radiation allows to produce highly sensitive, compact gamma cameras. This work addresses the needs of the first responder services to this threat by researching and improving contactless, robot assisted methods for the investigation procedures. The aim is to provide end users with reliable, fast and safe means to investigate IEDs and evaluate the imposed threat.

The material as well as the thickness of the sensor are deciding factors of the performance of a gamma camera. High Z semiconductor materials, such as Cadmium Telluride (CdTe), Cadmium Zinc Telluride (CdZnTe) and Thallium bromide (TlBr), offer fast analyzation of the investigated isotope due to their high absorption efficiency. The absorption efficiency can be further improved by increasing the thickness of the semiconductor sensor. However, the effect of charge sharing is increased accordingly [2 - 4]. Charge sharing describes the spreading of information from charge carriers over multiple pixels. The effect is heavily depended on the photon energy of the event and the thickness of the material due to the drift of charge carriers through the sensor layer. The main driving forces are repulsion between charge carriers and diffusion. Thicker sensors archive a higher attenuation efficiency which leads to superior energy resolution to identify the isotope, especially in the high energy region. A smaller pixel

size yields a better spatial resolution for localization of the isotope in the region of interest. A crucial aspect in the conception of a Gamma- or Compton camera lies in the dependence of absorption efficiency and the negative effect of the charge sharing on the spatial resolution.
In this work, four different ohmic sensor configurations were evaluated for the usage in a gamma camera. The material was supplied by Acrorad (Japan) while the flip-chip bonding was performed by the Freiburg Materials Research Centre (Germany). The 2 mm CdTe sensor was bonded to a Timepix1 readout chip with an increased pixel pitch of 110 μm. An increased pixel pitch (pp) counters the charge sharing effect on a hardware level at the detector side. The 0.45 mm, 1 mm and 3 mm CdTe detectors were connected to a Timepix1 readout with 55 μm pp. In this case, the 3 mm CdTe Timepix1 shows the highest effect of charge sharing but also provides the highest attenuation efficiency in photon energies above 100 keV (Fig. 1). Cluster analysis was performed for all detectors since all detector assemblies exhibit charge sharing regardless of configuration.

2. Materials and Methods

2.1. Cadmium Telluride

CdTe is an excellent semiconductor material for hard X-ray and gamma-ray detection. The high atomic number ($Z_{CdTe} \approx 50$) and density ($\varrho = 5.854$ g/cm³ at RT) provide superior attenuation efficiency above 30 keV compared to Si ($Z_{Si} = 14$) and GaAs ($Z_{GaAs} \approx 32$) and the wide bandgap energy ($E_{gap} = 1.44$ eV) permits the usage of the detector at room temperature without active cooling. The absorption efficiency can be enhanced furthermore by increasing the thickness of the material [5].

CdTe was considered and used as a semiconductor sensor for hybrid photon counting detectors (HPD) of the Medipix chipset family since the beginning of the Medipix collaboration. Previous work investigating the spectroscopic performance of a 1 mm CdTe sensor bump bonded to a Medipix2 chipset was presented by Maneuski et al. [6], Ruat and Ponchut [7] and Greiffenberg et al. [8]. Measurements regarding the characterization and spectroscopic performance of a Timepix1 chipset in combination with 2 mm CdTe [9, 10] and 3 mm CdTe [5] were shown recently. Cadmium Zinc Telluride (CdZnTe) is another promising semiconductor material in addition to CdTe. Recent work with CdZnTe sensors bump bonded to a Timepix1 chipset [11, 12] and performance investigations [13, 14] show encouraging results and are worth investigating in future work.

2.2. Timepix

The Timepix1 is a hybrid pixel detector (HPD) developed by the Medipix2 collaboration CERN [15]. It is fabricated in a CMOS 250 nm process, consists of 256 x 256 square pixels with a pixel pitch of 55 μm, resulting in a sensitive area of 1.98 cm².The detector provides three different counting modes [15]: single photon counting mode (Medipix Mode), Time-Of-Arrival Mode (ToA) and Time-over-Threshold Mode (ToT). For this work, all measurements were carried out using the Time-over-Threshold Mode (ToT).

The incoming signal is, individually for each of the 65536 pixels, amplified by a charge sensitive preamplifier and compared to a 4-bit threshold in the discriminator circuit which is connected to a synchronization logic. If the signal exceeds the threshold, a 14-bit counter is incrementing the number of clock units as long as the signal is above the threshold and below 11810 counts in which case the overflow logic stops. The number of incrementing clock pulse is proportional to the input charge and therefore to the photon energy of the event due to a linear discharge of the preamplifier controlled by the IKrum current. This contrasts with single photon counting pixel detectors which discharge using a resistor resulting in exponential decrease of the signal hub [16]. The energy threshold enables compensation of process variations.

Different semiconductor sensor materials like Si, CdTe, CdZnTe or GaAs can be connected to the Timepix ASIC and handled by the Krummenacher preamplifier which can process positive and negative charge inputs. The IKrum digital-to-analog-converter (DAC) (Figure 2) and has two functionalities: the compensation of leakage current and the discharge of the preamplifier feedback capacitor, which influences the duration of the return of the peak signal amplitude to the baseline. A

higher IKrum current leads to a faster discharge and thus shorter pulses which results in a reduction of pulse pileup but also to a reduction of signal amplitude, decreasing the energy resolution. The simulated dependence of the preamplifier output signal and width on the IKrum DAC settings are shown in [17].

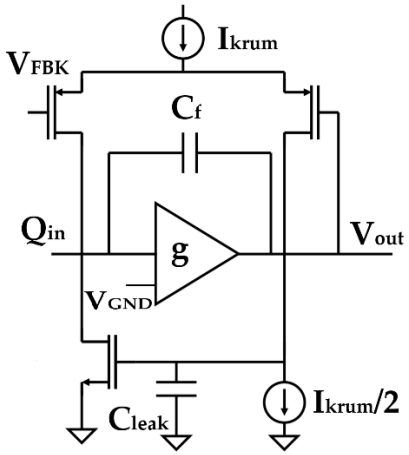

Figure 2. Schematic of the Krummenacher circuit. The IKrum current controls the leakage current compensation, in the case of electron collection IKrum/2, and the return of the signal to the baseline (adopted from [18, 17]).

The Timepix1 and its successor, the Timepix3, were initially aimed for particle detection. However, in recent years these detectors are used in medical imaging [19], space radiation dosimetry as well as in commercially available gamma cameras [20] and experimental Compton cameras [9, 21] with 1 mm and 2 mm CdTe sensor configurations.

2.3. From GAMPIX prototype to iPIX gamma camera

In order to address the need of instrumentation allowing the detection and location of radioactive materials, CEA List has been developing gamma camera systems for over thirty years [22]. These systems allow remotely visualizing gamma rays originating from radioactive emitters by superimposing a gamma image onto a visible image of the scene. Since the late 2000's, CEA List has been working on a new generation of gamma camera, which resulting prototype is called GAMPIX [23]. This prototype relayed on the use of a Timepix1 detector equipped with a 1 mm thick CdTe sensor, coupled with a coded mask ensuring the spatial modulation of incoming gamma flux Figure 3 (a).

Coded aperture is a technique of great interest, which allows achieving a good angular resolution for gamma source reconstruction, while maintaining a high sensitivity of the system. GAMPIX gamma camera is based on MURA coded masks, consisting in a mathematical arrangement of holes, defining the rank of the coded mask, into a denal collimator [24]. In the presence of radioactive sources, gamma-ray will go through holes and be stopped into denal, resulting in the projection of the MURA pattern on the gamma-sensitive sensor. The high pixelization of Timepix1-based detector allows accurately determining the location of gamma rays into the semi-conductor sensor, which ensures angular resolution of the overall imaging system. Indeed, the preferred pixel pitch of 55 μm ensures an achieved precision on pattern projection estimated around 0.20°, compared to 0.40° for a pixel pitch of 110 μm. This projection accuracy is a determining factor for the source location reconstruction. Moreover, the symmetry in the MURA pattern allows, by a 90° rotation of the coded mask, suppressing background noise, without any additional shielding. This feature, called anti-mask procedure, is of great interest in the case of measurements in areas subject to high gamma background while preserving lightness of the camera.

The GAMPIX prototype was validated in laboratory [25] and deployed in various real environments in the field of nuclear industry and Homeland Security applications [26]. Performance assessment of the gamma camera prototype showed that the system was able to perform imaging measurements in a field

of view of 50° with an angular resolution ranging from 1.35° to 3.81° depending on the pattern of coded mask used. As presented in Table 1, the sensitivity of the prototype makes it possible to visualize sources in less than a minute over the whole range of energies encountered in the field of nuclear industry (i.e. from ^{241}Am at 59.5 keV to ^{60}Co at 1.33 MeV) [26].

Table 1. Sensitivity of GAMPIX gamma camera, according to the rank of the mask (R7 is for rank 7, R13 for rank 13, e2, e4, e8 indicates the corresponding thickness in mm) and to the nature of the radioactive source. The dose rate was measured in the vicinity of the gamma camera.

Radionuclide	Dose rate ($\mu Sv.h^{-1}$)	R13 – e2	R7 – e4	R7 – e8
^{241}Am	0.25	3 s	1 s	1 s
^{137}Cs	2.50	300 s	60 s	20 s
^{60}Co	3.84	Not detected	400 s	60 s

From 2010, CEA List started the industrial transfer of GAMPIX prototype toward CANBERRA, now MIRION Technologies. The resulting commercial system, called iPIX and pictured on Figure 3 (b), is based on the same technology as GAMPIX [27]. This commercial version was completely redesigned for compactness (L × l × P = 9 cm × 9 cm × 18.85 cm) and shielding was optimized for improving system weight (2.5 kg). The anti-mask procedure was automated, and the connection simplified using Power-over-Ethernet method for simultaneous communication and power supply purpose.

(a) **(b)**

Figure 3. (a) Picture of GAMPIX second-generation gamma camera developed by CEA List; (b) Picture of iPIX gamma camera, industrialized version of GAMPIX and commercialized by MIRION Technologies.

3. Results

A sufficient bias was applied to all investigated detector assemblies during the presented measurements to ensure full charge collection efficiency. This was verified by measuring the count rate of the detector versus increasing sensor bias voltage under identical X-ray tube settings. The maximum charge collection efficiency is achieved when the count rate reaches saturation. The leakage current was measured before the experiments with no radiation present (Table 2). The high leakage current of the 0.45 mm CdTe is due to the effect of the processing of the thin material. A new dicing process was implemented which permits significant cleaner edges of the bonded sensor. The improved performance of this process can be seen in the low leakage currents of the 1 mm and 3 mm thick detector assemblies. In the case of the 2 mm sensor, the observed increase in leakage current is due to

an earlier bonding date of the detector assembly. There is no surface preservation on the as-diced chip edge. Over time, degradation effects occur which lead to greater surface leakage currents.

Table 2. Detector settings and configurations used for the measurements of 3.1 and 3.2.

Sensor thickness	Bias (V)	Leakage current (μA)	Pixel pitch (μm)
3 mm CdTe	-1200	2.5±0.2	55
2 mm CdTe	-600	8 ±1.2	110
1 mm CdTe	-450	2.1±0.2	55
0.45 mm CdTe	-230	43±4	55

The DAC for leakage current compensation (IKrum) and the clock frequency were set to the same value for all assemblies to ensure comparable results regarding the spectroscopic performance (Table 2). All measurements were taken with a clock frequency of 9.6 MHz and IKrum 5 which corresponds to an IKrum current of roughly ~7.5 nA [15]. At IKrum 5, the mean pulse duration of a 100 keV photon is ~6 μs [18]. All detectors passed stability measurements with radiation present and continues operation in the range from 12 to 24 hours with the configurations shown in Table 2.

Even while performing cluster analysis, the charge sharing effect has a strong influence on the energy resolution of the sensor. This is caused by the limited rise time of the preamplifier in the pixel cell and the higher number of pixels marking the edge of the cluster, which have deposited energy of the event, but the threshold was not exceed. This, so called dead energy, has a greater impact on the energy resolution with increasing cluster size of the event since more surrounding pixels exhibit the dead energy effect.

3.1. Spectroscopic Performance

The common radioactive sources ^{137}Cesium (^{137}Cs), ^{152}Europium (^{152}Eu) and ^{60}Cobalt (^{60}Co) are investigated by the different detector assemblies in a laboratory environment. All detectors were calibrated by the noise edge method [28] in Pixelman 2.2.3 [29]. The acquisition time was determined for each setup individually to minimize event pile up. Since the thickest sensor exhibits the highest attenuation efficiency, a time was chosen with, on average, 5 events per frame for the 3 mm CdTe detector. All measurements were performed in a fixed timeframe of 1000 s and a fixed distance from source to detector of 60 mm. Cluster analysis was performed for each measurement which identifies counting pixels exhibiting charge sharing as well as separated fluorescence photons and contributes them to their original event. Gaussian fitting is used for the primary gamma ray line of each spectrum and the sigma (σ) is calculated with σ = w/2. Fig. 4, Fig. 5 and Fig. 6 show the measured spectra for ^{137}Cs, ^{152}Eu and ^{60}Co. The raw spectra were normed in ToT-value on the x-axis a distinguished feature in the spectrum were adjusted to the correlated energy because the TOT values differ per detector. The spectra are superimposed on each other to visualize the difference in performance. All spectra were smoothed by moving average of 10 and the count rate was normalized.

The relative absorption efficiency of all sensors was evaluated in comparison to the 3 mm CdTe sensor which exhibits the greatest attenuation efficiency. Previous work investigated the relative absorption efficiency of 1 mm and 0.45 mm CdTe sensors [5]. The data was corrected for the different number of inactive pixels per sensor caused by crystal inhomogeneities and degenerating effects like corner peel. The measurement error was calculated by Gaussian error propagation law.

3.1.1. Cesium-137

^{137}Cs is an isotope used in the medical environment for radiation therapy. Therefore, in the context of the evaluation of the performance of a gamma camera. The acquisition time was set to 10 ms for all

detectors. The lab source has an activity of 3.58 ± 0.09 MBq at the time of the experiment. Figure 4 presents the measured spectra of ^{137}Cs with the different detector assemblies.

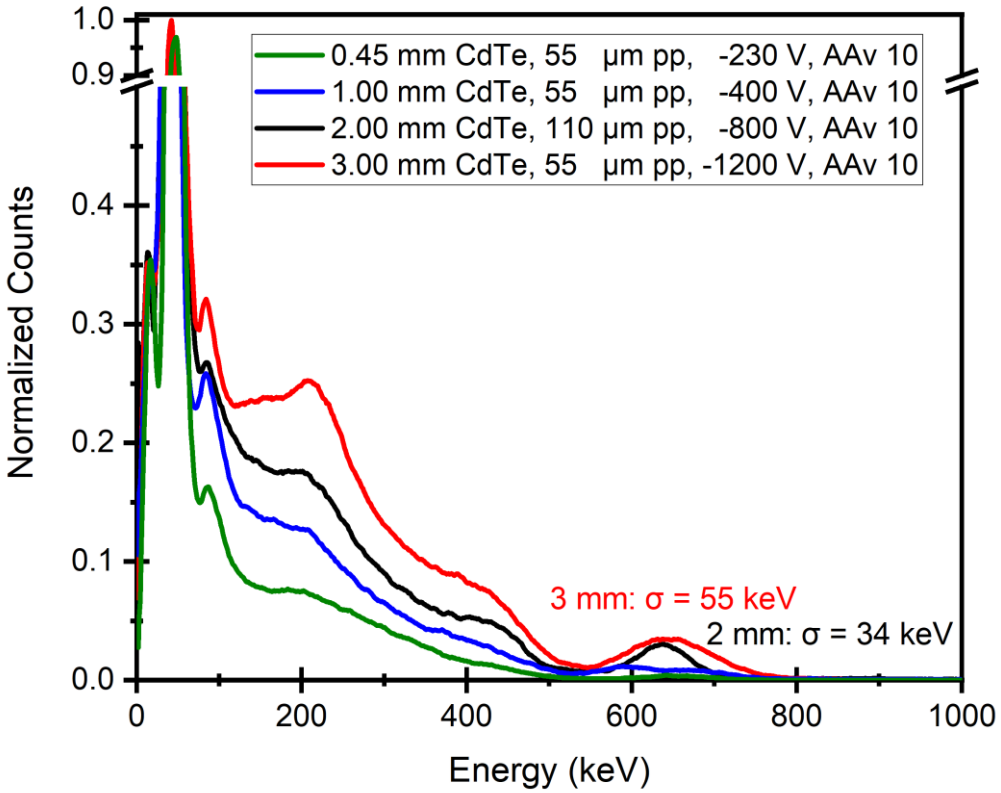

Figure 4. Spectra of ^{137}Cs investigated by four different detector configurations in this work. The sigma of the gamma ray line at 667 keV is shown.

The characteristic gamma ray line of ^{137}Cs at 667 keV can be identified with all investigated detector configurations with a significant correlation in amount of counts and attenuation efficiency of the different sensors. A sigma of 55 keV is achieved for the gamma ray line in the case of the 3 mm CdTe sensor which exhibits the strongest charge sharing of all configurations caused by the thickness of the sensor layer and the 55 µm pixel pitch. In direct comparison, the 2 mm CdTe sensor shows, with greater 110 µm pixel pitch, a decreased sigma of 34 keV resulting in a more defined peak of the gamma ray line. The 0.45 mm CdTe sensor exhibits a comparable sigma to the 2 mm CdTe configuration. This is achieved by the significant thinner sensor material which results in less charge sharing and a comparable energy resolution even with a 55 µm pixel pitch. Besides the Ba L X-ray line of the source at 32 keV another peak is visible in all four spectra at 75 keV. This peak corresponds to the Pb k-edge energy ($K_{\alpha 1}$ 75 keV) and is originating from the Pb enforced shielding in the measurement environment.

A relative absorption efficiency of (0.370 ± 0.003) for 0.45 mm CdTe, (0.544 ± 0.002) for 1 mm CdTe and (0.801 ± 0.002) for 2 mm CdTe in comparison to the 3 mm CdTe was measured.

3.1.2. Europium-152

^{152}Eu is a gamma and beta emitter used in hard-gamma brachytherapy. At the time of the measurement, the lab source had an activity of 0.28 ± 0.01 MBq. The set acquisition time for all sensors was 32 ms, which was chosen to minimalize event pile up. Figure 5 shows the ^{152}Eu spectra measured by the four investigating detector configurations.

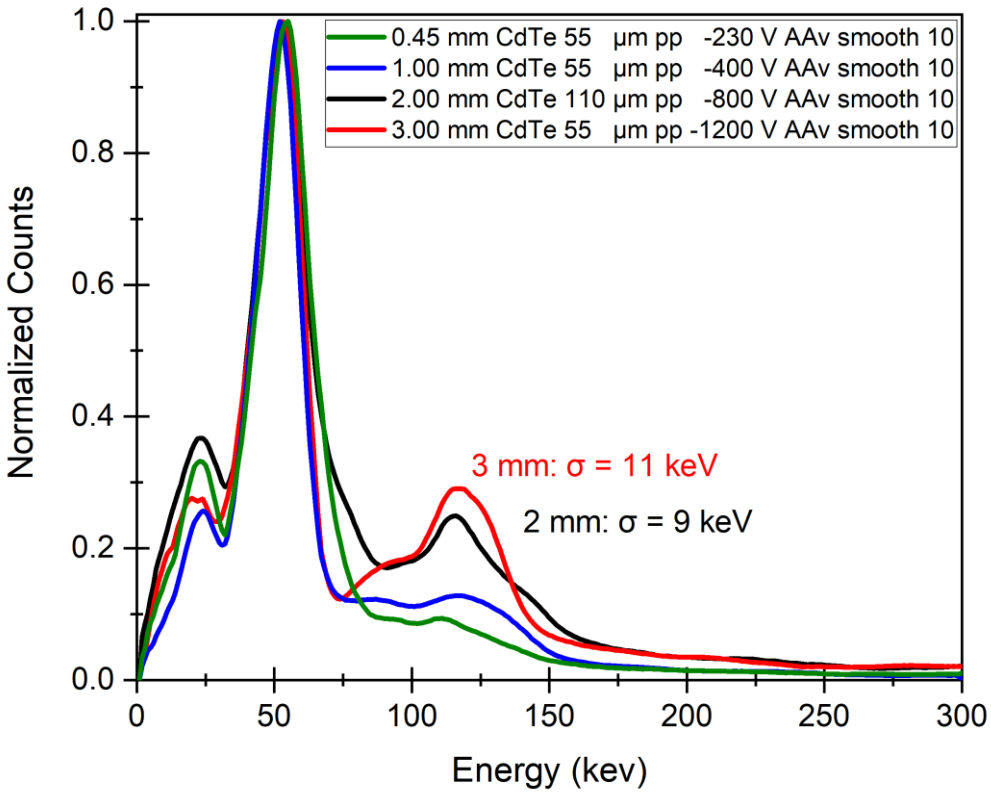

Figure 5. Spectra of ^{152}Eu investigated by four different detector configurations in this work. The sigma of the gamma ray line at 122 keV is shown.

The ^{152}Eu isotope exhibits a characteristic gamma ray line at 122 keV which is resolved with a sigma of 11 keV in the case of the 3 mm CdTe sensor configuration with 55 µm pixel pitch. As with the characteristic ^{137}Cs gamma ray line, the 2 mm CdTe sensor with 110 µm pixel pitch shows an improved sigma of 9 keV. The 1 mm and 0.45 mm sensors show a significantly less distinguishable peak at 122 keV caused by a reduced attenuation efficiency at the corresponding energy.

For ^{152}Eu, the difference in absorption efficiency between the investigated sensors is less evident than for ^{137}Cs and ^{60}Co. This is due to the Sm L-lines at 40 keV (Sm $K_{\alpha 1}$) and 39 keV (Sm $K_{\alpha 2}$), originating from the ^{152}Eu decay chain, which have an absorption efficiency above 99 % for all investigated sensors. In addition, the emitted beta particles of ^{152}Eu are absorbed in the first few µm of the sensor layer regardless of the thickness. However, multiple gamma ray lines at energies >200 keV contribute to the observed ratio in relative absorption efficiency compared to the 3 mm sensor of (0.637 ± 0.003) for 0.45 mm CdTe, (0.777 ± 0.003) for 1 mm CdTe and (0.944 ± 0.003) for 2 mm CdTe.

3.1.3. Cobalt-60

^{60}Co is used in medical radiotherapy as a radiation source and therefore common in most hospitals and a potential isotope in an IED. In this investigation, it is used to evaluate the spectroscopic performance of the detectors for high energy photons since ^{60}Co exhibits two characteristic gamma ray lines at 1173 keV and 1333 keV. At the time of the experiment, the used lab source had an activity of 6.55 ± 0.16 Mbq. The acquisition time was set to 5 ms. Figure 6 presents the measured spectra of ^{60}Co investigated by the different detector assemblies in this work.

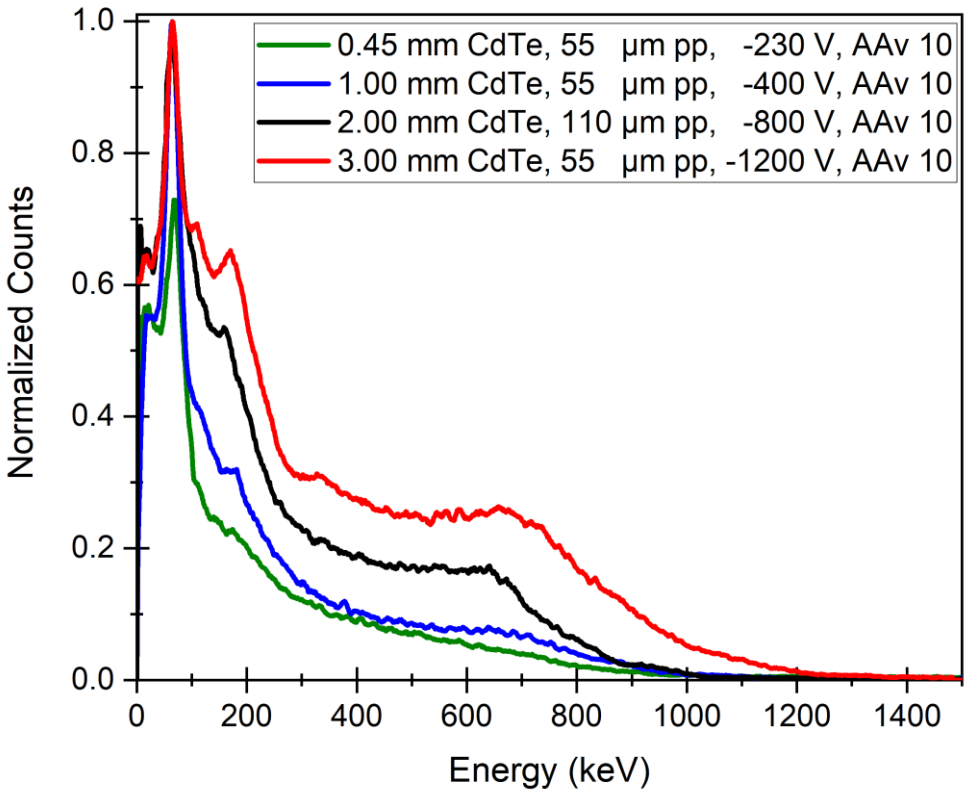

Figure 6. Spectra of ^{60}Co investigated by four different detector configurations in this work.

No photo peak of the gamma ray lines at 1173 keV and 1333 keV can be distinguished regardless of detector configuration. This is due to the presence of undetected escape photons originating from the predominant Compton scattering, the limited energy resolution of the Timepix1 detector and the low attenuation efficiency of ~ 8.8% in the case of the 3 mm CdTe sensor. An even thicker sensor would be desirable for ^{60}Co. A significant reduction in overall count rate can be overserved for the 1 mm and 0.45 mm sensors. As with the ^{137}Cs spectrum, the Pb ($K_{\alpha 1}$ 75 keV) is visible.

A significant reduction in overall count rate can be overserved for the 1 mm and 0.45 mm sensors with a relative absorption efficiency of with (0.238 ± 0.002) for 0.45 mm CdTe and (0.396 ± 0.004) for 1 mm CdTe compared to the 3 mm CdTe. The 2 mm CdTe sensor exhibits the same effect as the thinner sensors but to a lesser degree with a relative absorption efficiency compared to the 3 mm sensor of (0.641 ± 0.005).

3.3. Implementation and field testing

After investigating the spectroscopic performance in chapter 3.1 and 3.2, a field test campaign was initiated to evaluate the influence of a thicker sensor on the localization capabilities of the gamma camera. The 3 mm CdTe sensor has the highest attenuation efficiency of the investigated sensors and the 55 µm pixel pitch permits the necessary spatial and angular resolution for the localization of the threat. Therefore, a 3 mm CdTe Timepix1 detector assembly with 55 µm pixel pitch was implemented in the iPIX gamma camera. Figure 7 shows the camera mounted on the robot Telemaxx manufactured and provided by Telerob GmbH (Germany). A specific mounting solution of the gamma camera was provided by ZIPPERMAST GmbH (Germany) which mounts the iPIX on the robotic arm. Following

this approach, it was possible to remain the manipulation capabilities of the robot on investigating objects while having a 360° radius for the FOV of the gamma camera.

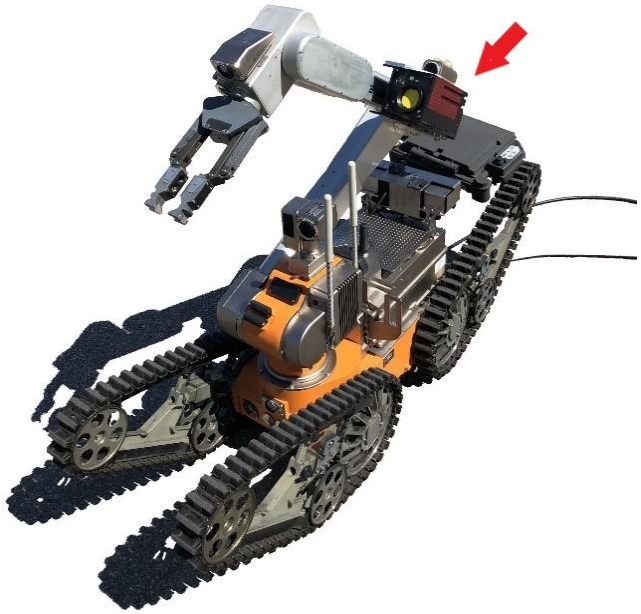

Figure 7. Telemaxx by Telerob with the iPIX mounted on the arm. The mounting method does not negatively influence the manipulation ability of the robot while permitting at the same time a 360° radius for the position of the gamma camera.

3.3.1. NBC testing side

During the project, it was possible to carry out a field test of the modified iPIX at the NBC testing side of the Austrian army at the DABSCH Kaserne (Austria). A room was prepared for investigation with a simili, containing a radioactive source, placed inside. The complete system could be tested under realistic conditions outside the lab environment [30]. Figure 8 (a) shows the superimposed image of the gamma camera with localized radiation source in a suitcase. ^{137}Cs is the investigated isotope with an activity of 36 ± 0.9 Gbq. The distance from source to detector was 1.7 meters with 218 recorded counts per second (Cps). Figure 8 (b) presents the spectrum which was simultaneously recorded in 100 seconds.

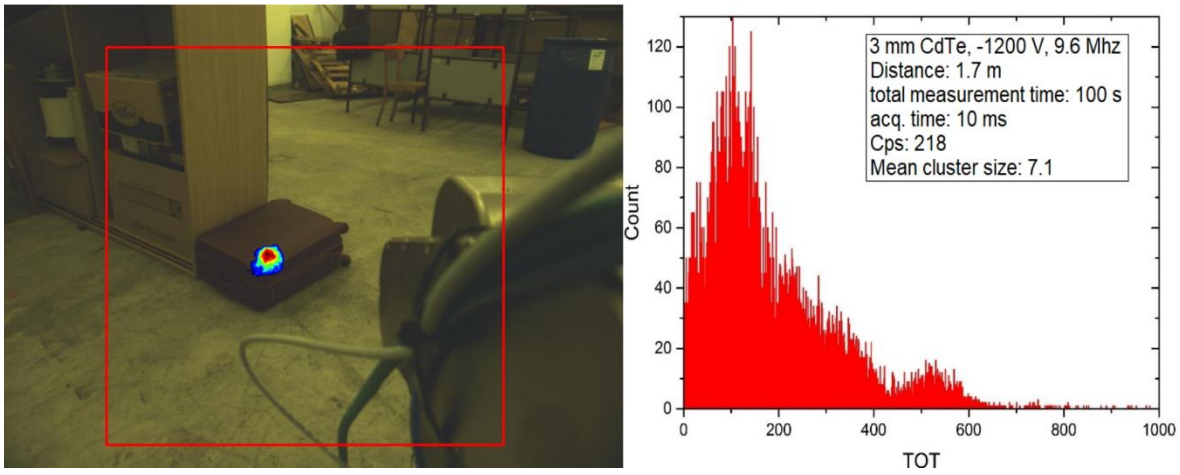

(a) **(b)**

Figure 8. (a) Investigation of a prepared smili at the NBC testing side. A ^{137}Cs source with an activity of 36 ± 0.9 Gbq is placed inside and localized by the 3 mm CdTe sensor with 218 Cps. (b) The spectrum which was recorded at the same position in 100s. The mask R7 – e4 (Table 1) was used for the measurement.

In comparison to the normalized ^{137}Cs spectrum measured in the lab, shown in Figure 4, the raw ToT-values are presented on the x-axis in Figure 8 (b). A total measurement time of 100s was chosen since it represents a realistic time frame to investigate a suspicious object in case of an emergency situation regarding the potential isotope present. The overall spectrum is noisier which is a result of the lower event count. However, the gamma ray line at 662 keV can be distinguished.

3.1.2. Nuclear Powerplant test facility

A second field test was performed with the iPIX configuration described in section 3.3 at a nuclear power plant test site. A ^{60}Co source was placed inside a test structure which is 150 cm wide and 100 cm in height. Three tubes are in equal distance and the isotope is placed randomly in one arm. The source has an activity of 2.8 ± 0.07 Gbq which corresponds to a dose rate of ~1 mSv/h in 1 m distance. Table 3 shows the results of the measurements. Figure 9 presents the distance 25 meters (a) and 20 meters (b). Figure 10 shows the distance 15 meters (a) and 12 meters (b) respectively. The attenuation efficiency of the 3 mm CdTe sensor in the energy region of ^{60}Co enables a timely localization of the test object with a maximum of 200 s in the case of 25 meters distance. It was possible to visually localize the isotope in the right arm of the structure at 20 meters.

Table 3. Distance measurement at the nuclear power plant test facility. The isotope ^{60}Co with an activity of 2.8 ± 0.07 Gbq is investigated. The visible localization is the ability of the user to identify the radioactive source placed inside the right arm of the test structure on the superimposed image of the iPIX.

Distance (m)	Cps	Acquisition time (s)	Visible localization
25	13.2	200	No
20	21.5	116	Yes
15	37.1	91	Yes
12	43.8	72	Yes

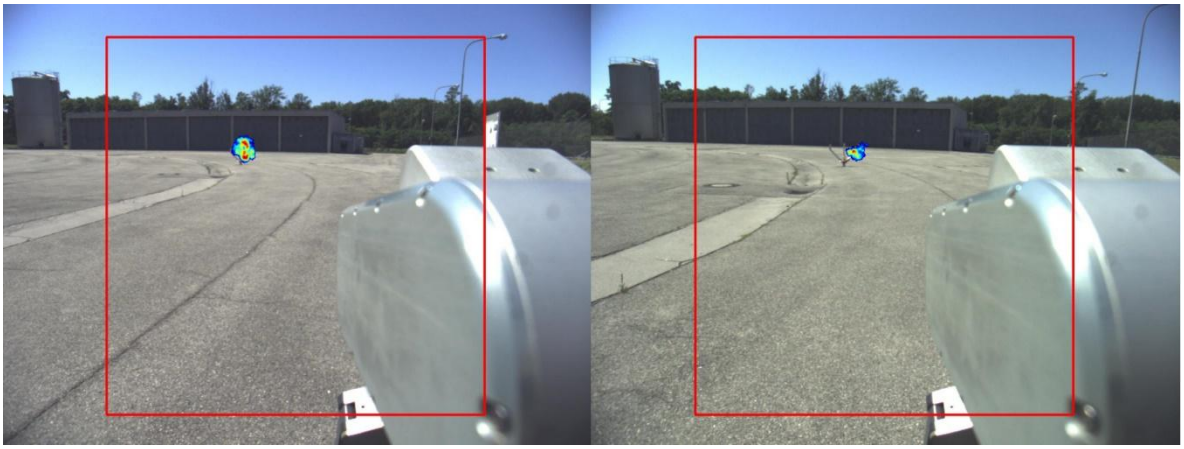

(a) **(b)**

Figure 9. A ^{60}Co source with an activity of 2.8 ± 0.07 GBq (dose rate of ~ 1 mSv/h in 1 m distance) is placed in a structure which is 100 cm in height and 150 cm wide with three tubes in equal distance from each other. In (a), the distance between source and gamma camera is 25 meters. The sensor registered 13.2 Cps and the superimposed image was taken with an acquisition time of 200 s. It is not possible to identify the tube with the source. In (b), the

distance between source and camera was reduced to 20 meters resulting in 21.5 Cps. It is possible to identify the right tube as the source of radiation with 116 s acquisition time.

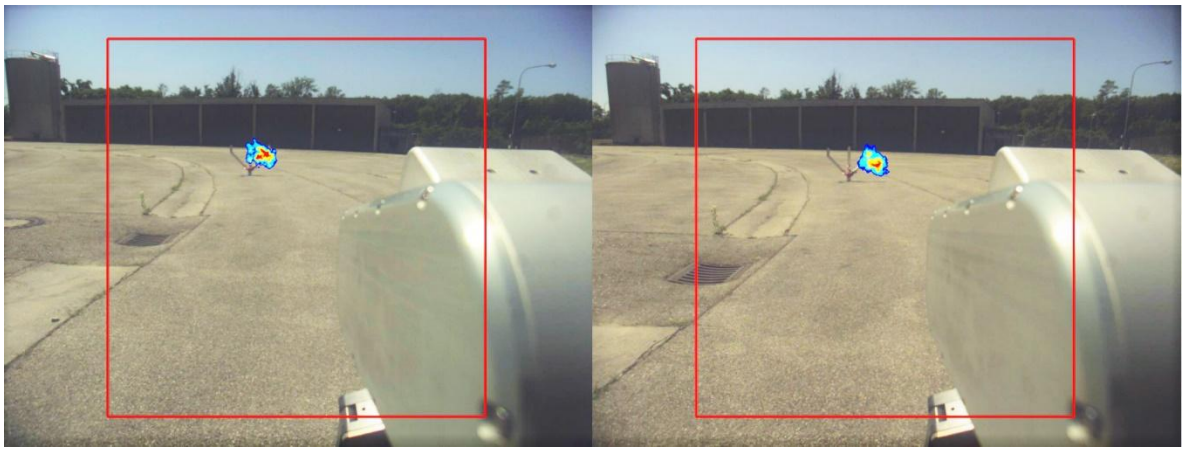

(a) (b)

Figure 10. The distance of detector and source is reduced to 15 meters in (a) and 12 meters in (b). In both cases, it can be determined visually that the source is placed in the right arm of the structure. For the 15 meters distance, 37.1 cps with an acquisition time of 91 s were evaluated. The right image with 12 meters distance yield 43.8 cps with an acquisition time of 72 s.

A spectrum was recorded at 15 meters distance between the ^{60}Co source and detector shown in Figure 11. The total measurement time was 50 s due to on-site time restrictions. The spectrum is noisier than the spectrum in the lab environment. This is expected due to the distance of 15 meters to the source resulting in a low count rate. The information would not be feasible to identify the investigated isotope, however, the presence of high energy photons can be determined since the cluster analysis detects and sufficiently excludes alphas and muons from the evaluation [5].

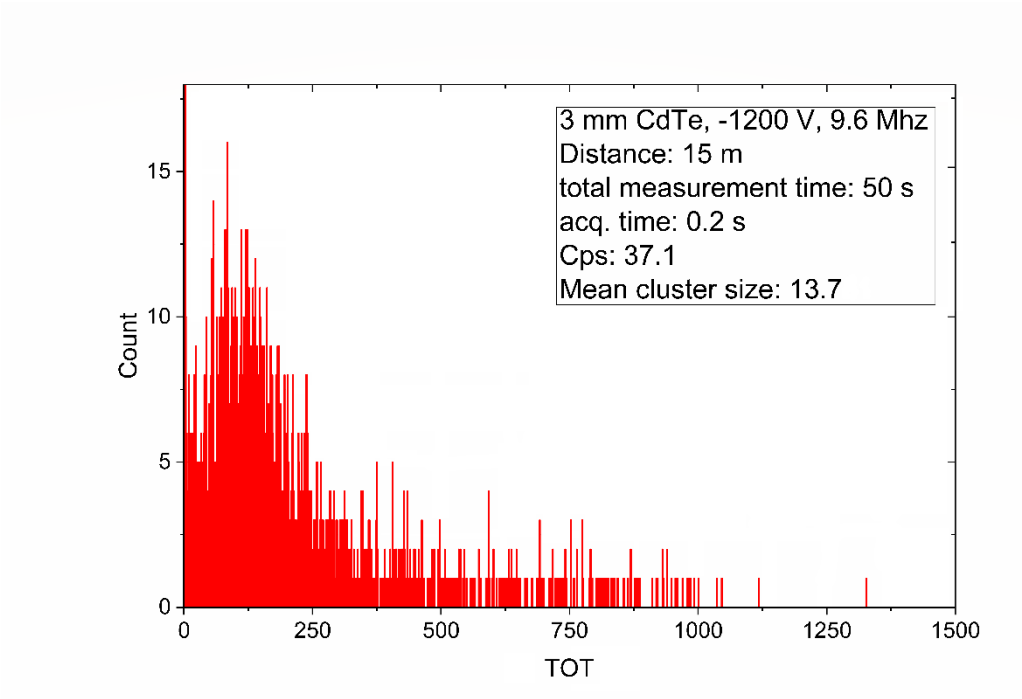

Figure 11. ^{60}Co spectrum recorded during the measurement series at the nuclear power plant test facility. The distance between source and detector is 15 meters with a total measurement time of 50 s. The mask R7 – e4 (Table 1) was used for the measurement.

A test parkour was prepared inside the power plant which is designed to evaluate the maneuverability and manipulation capabilities of the robot as well as localization of hidden radioactive sources. Video 1 shows a short clip of the iPIX mounted on the Telemaxx at the parkour during ENRICH 2019 (Austria).

Supplementary Material Video

Video 1. This video shows the Telemaxx bomb disposal robot with the iPIX mounted on the side arm during ENRICH 2019 (Austria). The iPIX used the 3 mm CdTe detector configuration. The parkour is designed to test the maneuverability and manipulation possibilities of the robot. In addition, radioactive sources must be localized.

3.4. Comparison to related work in the field

The presented approach uses the small pixel pitch of the Timepix ASIC and cluster analysis to guarantee a high angular resolution of the gamma camera by means of the MURA coded aperture as well as to provide spectroscopic information. A comparable gamma camera design approach is the Caliste-HD [31], which uses a CdTe hybrid detector with a 16 x 16 pixel matrix with 580 µm pixel pitch and MURA coded mask for the localization capabilities. The pixel size used in Caliste-HD is much higher than in the IPix to reduce charge sharing effects without performing a cluster analysis. The relation of sensor thickness to pixel pitch enables the evaluation of single pixel events only for spectroscopic investigation. This results in a superior energy resolution. The gamma ray line of ^{152}Eu at 121 keV is resolved with a sigma of 0.9 keV in comparisons to the sigma of 11 keV of the 3 mm CdTe Timepix used in this work. However, as both coded-aperture imaging systems use a MURA mask, the highly pixelated Timepix has an angular resolution ranging from 1.3° to 3.8°, depending on the isotope, while the Caliste-HD system is reporting an angular resolution of only 7° in the case of ^{152}Eu [31].
Scintillator based gamma cameras show a 6.0° angular resolution at 356 keV with a $LaCl_3$(Ce) scintillator consisting of 22 x 22 voxels using URA coded aperture [32] and 5.6° angular resolution with a CsI (Na) detector module consisting of 20 x 20 voxels using a MURA coded aperture [34].
The CsI (Na) compact hybrid gamma camera was used to investigate the position of UO_2 pellets with 4.1 % enriched ^{235}U and an activity of 1.14 µCi [34]. The results were used to predict the minimum required detection time and count rate for monitoring different amounts of UO_2 pellets at 10-meters distance between source and detector. A localization time of 199.4 s and a count rate of 30.9 cps was found feasible to use the CsI (Na) compact hybrid gamma camera in the proposed scenario. In this work, it was possible to localize a ^{60}Co source in 20-meters distance in 116 s with a significant lower count rate per second of 21.5 Cps. The estimated required time of localization in a time crucial situation agrees with the localization times stated in this work.
A single layer Compton camera is another camera concept which uses Compton scattering for isotope localization by reconstructing the scattering angle [35]. The advantage to renounce the coded-aperture system enables the construction of smaller and lighter camera systems. However, since the localization principle relies on Compton scattering, the detection efficiency of the camera is declining with decreasing energy of the investigated isotope. Furthermore, the distance between source and camera has to be known for position identification.
Recently, a hybrid Compton camera was proposed, combing a classical Compton camera and a pinhole camera in a single detector system. This hybrid camera achieves a sigma of 3.5 keV at the gamma ray line of ^{137}Cs at 662 keV, in comparison to sigma 55 keV of the 3 mm Cdte Timepix, and an angular resolution of 10° [36].

. Discussion and Conclusions

Four different CdTe sensor configurations were bonded on Timepix1 readout ASIC to evaluate the spectroscopic performance for the integration in a gamma camera used on a robotic platform for counter measurements for radioactive threats.

Energy resolution is systematically better with greater pixel size and thinner sensors due to less charge sharing present. The 2 mm CdTe 110 μm pp detector exhibits a sigma 34 keV for the ^{137}Cs gamma ray line at 662 keV compared to sigma 55 keV for the 3 mm CdTe 55 μm pp detector. A negative influencing factor on the energy resolution is the deposition of not registered energy around a cluster due to the threshold of the individual pixel cell. This effect increases with overall cluster size due to a greater number of surrounding pixels. However, the attenuation efficiency of a sensor is an important aspect for a gamma camera since it allows efficient charge collection for a fast localization of the radioactive source especially for high energy gamma rays which pose an extensive threat to public safety. For the common isotope ^{137}Cs, the 3 mm CdTe sensor shows increase in count rate up to a factor of 1.25 compared to a 2 mm CdTe sensor, 1.84 compared to a 1 mm CdTe sensor and up to 2.71 compared to a 0.45 mm CdTe sensor (Fig. 4, ^{137}Cs).

In a scenario in which the possible source of radiation is unknown to the user, the extension of the field of view (FOV) of the camera by means of the possible distance between source and detector enables the first assessment of the situation in a timely matter. This depends on the attenuation efficiency and angular resolution of the detector. The integrated 3 mm CdTe detector measured 21.5 counts per second emitting from a ^{60}Co source with an activity of 2.8 ± 0.07 Gbq in 20-meters distance in an open environment. The acquisition time with visual identification by the user was 116 seconds.

The relative absorption efficiency measured in section 3.2 allows the calculation of the estimate acquisition time of a 1 mm CdTe sensor in the same scenario. In 20-meters distance from the source, the 1 mm CdTe sensor would have a predicted 8.5 cps resulting in 293 s acquisition time. For the intended use of the gamma camera to assisted in situations where the public safety is concerned, the time difference in localization of the source is significant for immediate decisions on appropriate countermeasures. The angular resolution was sufficient for the user to localize the radioactive isotope inside the test structure without knowing the placement for this measurement. At a 25-meters distance between detector and source, it was not possible for the user to distinguish the placement of the source inside the test structure.

A teleoperated robot platform with manipulation capabilities in combination with a gamma camera can assist police, fire workers and personal from nuclear powerplants in hazard and security operations. It poses the prospect to position the user and personal in a safe distance from a radioactive threat while, at the same time, remain the possibilities of interaction with the investigated object. Furthermore, in the frequent case of non-attacks, in which suspicious objects turn out to be harmless, the 3 mm CdTe sensor improves investigation speed significantly compared to the 1 mm CdTe sensor. For future work, it is worth investigating even thicker CdTe sensors in combination with highly pixelated ASICs such as the Timepix1 as well as other high Z sensor materials such as CdZnTe and TiBr which have similar or superior attenuation efficiency as CdTe while are available in greater sensor thickness.

Author Contributions: Conceptualization, J.F. and S.P.; methodology, J.F. and S.P.; software, J.F. and S.P.; validation, M.K.S., J.S.U. and J.F.; formal analysis, J.F.; investigation, J.F. and M.K.S.; resources, M.F., F.C., A.F. and V.S.; data curation, , M.K.S., J.S.U. and J.F.; writing—original draft preparation, J.F., S.P. and V.S.; writing—review and editing, J.F.; visualization, J.F.; supervision, S.P. and M.F.; project administration, S.P. and M.F.; funding acquisition, M.F.. All authors have read and agreed to the published version of the manuscript.

Funding: This research was funded by the German Federal Ministry of Education and Research (BMBF), grant number 13N14328.

Acknowledgments: The authors would like to express their thanks to all collaborations partners of project "DURCHBLICK" (BMBF, grant no. 13N14328) in particular Andreas Ciossek of Telerob GmbH (Germany) for providing the robot and Frank Woodcock of ZIPPERMAST GmbH (Germany) for manufacturing the mounting solution of the iPIX. We would like to thank the Fraunhofer FKIE (Germany), the Bundesheer (Austria) and the organizers of the ENRICH for the opportunity of on-site testing of the system.

Conflicts of Interest: The authors declare no conflict of interest.

References

1. van Ballegooij, W; Bakowski, P. The fight against terrorism. Study by European Parliamentary Research Service, PE 621.817 - May 2018. Available online: https://www.statewatch.org/media/documents/news/2018/may/ep-study-terrorism-cost-of-non-europe-5-18.pdf (accessed on 23.09.2020)
2. Mathieson, K.; Passmore, M.S.; Seller, P.; Prydderch, M.L.; O'Shea, V.; Bates, R.L.; Smith, K.M.; Rahman, M. Charge sharing in silicon pixel detectors, *Nucl. Instrum. Methods Phys. Res. A* ***2002***, *487*, pp. 113-122.
3. Korn, A.; Firsching, M.; Anton, G.; Hoheisel, M.; Michel, T. Investigation of charge carrier transport and charge sharing in X-ray semiconductor pixel detectors such as Medipix2, *Nucl. Instrum. Methods Phys. Res. A* ***2007***, *576*, pp. 239–242, doi: 10.1016/j.nima.2007.01.159.
4. Veale, M.C.; Bell, S.J.; Duarte, D.D.; Schneider, A.; Seller, P.; Wilson, M.D.; Iniewski, K. Measurements of charge sharing in small pixel CdTe detectors, *Nucl. Instrum. Methods Phys. Res. A* ***2014***, *767*, pp. 218–226.
5. Fey, J.; Procz, S.; Schütz, M. K.; Fiederle, M. Investigations on performance and spectroscopic capabilities of a 3 mm CdTe Timepix detector. *Nucl. Instrum. Methods Phys. Res. A* ***2020***, *977*, p. 164308, doi: 10.1016/j.nima.2020.164308.
6. Maneuski, D.; Astromskas, V.; Frojdh, E.; Frojdh, D.; Gimenez, E.N.; Marchal, J.; O'Shea, V.; Stewart, G.; Tartoni, N.; Wilhelm, H.; Wraight, K.; Zaina, R.M. Imaging and spectroscopic performance studies of pixellated CdTe Timepix detector, *J. Instrum.* ***2012***, *7 (C01038),* p. C01038, doi: 10.1088/1748-0221/7/01/C01038.
7. Ruat, M.; Ponchut, C. Characterization of a Pixelated CdTe X-Ray Detector Using the Timepix Photon-Counting Readout Chip, *IEEE Trans. Nucl. Sci.* ***2012***, *59*, pp. 2392–2401, doi: 10.1109/TNS.2012.2210909.
8. Greiffenberg, D.; Fauler, A.; Zwerger, A.; Fiederle, M. Energy resolution and transport properties of CdTe-Timepix-Assemblies, *J. Instrum.* ***2011***, *6 (C01046)*, p. C01046, doi: 10.1088/1748-0221/8/05/C05003.
9. Turecek, D.; Jakubek, J.; Trojanova, E.; Sefc, L.; Kolarova, V. Application of Timepix3 based CdTe spectral sensitive photon counting detector for PET imaging, *Nucl. Instrum. Methods Phys. Res. A* ***2018***, *895*, pp. 84-89, doi: 10.1016/j.nima.2018.04.007.
10. Bergmann, B.; Burian, P.; Manek, P.; Pospisil, S. 3D reconstruction of particle tracks in a 2 mm thick CdTe hybrid pixel detector, *Eur. Phys. J. C* ***2019***, pp. 79 165, doi: 10.1140/epjc/s10052-019-6673-z.
11. Tsigaridas, S.; Ponchut, C. X-ray imaging with high-Z sensors for the ESRF-EBS Upgrade, *J. Instrum.* ***2019***, *14 (C04009),* p. C04009, doi: 10.1088/1748-0221/14/04/C04009.
12. Tsigaridas, S.; Ponchut, C.; Zanettini, S.; Zappettini, A. Characterization of pixelated CdZnTe sensors using MAXIPIX, *J. Instrum.* ***2019***, *14 (C12009),* p. C12009, doi: 10.1088/1748-0221/14/12/C12009.
13. Veale, M.C.; Booker, P.; Cross, S.; Hart, M.D.; Jowitt, L.; Lipp, J.; Schneider, A.; Seller, P.; Wheater, R.M.; Wilson, M.D.; Hansson, C.C.T.; Iniewski, K.; Marthandam, P.; Prekas, G. Characterization of the Uniformity of High-Flux CdZnTe Material. *Sensors* ***2020***, *20*, p. 2747, doi: 10.3390/s20102747.
14. Thomas, B.; Veale, M.C.; Wilson, M.D.; Seller, P.; Schneider A.; Iniewski, K. Characterisation of Redlen high-flux CdZnTe, *J. Instrum.* ***2017***, *12 (C12045),* p. C12045, doi: 10.1088/1748-0221/12/12/C12045.
15. Cudié, X.L. Design and characterization of 64K pixels chips working in single photon processing mode, Ph.D. thesis, Sundsvall Mittuniversitetet, 2007.
16. Johnson, I.; Bergamaschi, A.; Billich, H.; Cartier, S.; Dinapoli, R; Greiffenberg, D.; Guizar-Sicairos, M.; Henrich, B.; Jungmann, J.; Mezza, D.; Mozzanica, A.; Schmitt, B.; Shi, X.; Tinti, G. Eiger: a single-photon counting x-ray detector. J. Instrum. 2014, 9 (C05032), p. C05032, doi: 10.1088/1748-0221/9/05/C05032.
17. Hamann, E.; Koenig, T.; Zuber, M.; Cecilia, A.; Tyazhev, A; Tolbanov, O.; Procz, S.; Fauler, A.; Fiederle, M.; Baumbach, T. Investigation of GaAs:Cr Timepix assemblies under high flux irradiation. J. Instrum. 2015, 10 (C01047), p. C01047, doi: 10.1088/1748-0221/10/01/C01047.
18. Llopart, X.; TimePix manual v1.0, CERN 2006.
19. Procz, S.; Avila, C.; Fey, J.; Roque, G.; Schuetz, M.; Hamann, E. X-ray and gamma imaging with Medipix and Timepix detectors in medical research. Radiat. Meas. 2019, 127, p. 106104, doi: 10.1016/j.radmeas.2019.04.007.
20. Amgarou, K.; Paradiso, V.; Patoz, A.; Bonnet, F.; Handley, J.; Couturier, P.; Becker, F.; Menaa, N. A comprehensive experimental characterization of the iPIX gamma imager, J. Instrum. 2016, 11 (P08012), p. P08012. doi: 10.1088/1748-0221/11/08/P08012.
21. Amoyal, G. Development of a hybrid gamma imager for nuclear industry applications, PhD Thesis, CEA List, 2019.

22. Gal, O.; Izac, C.; Jean, F.; Laine, F.; Leveque, C.; Nguyen, A. CARTOGAM – a portable gamma camera for remote localization of radioactive sources in nuclear facilities. Nucl. Instrum. Methods Phys. Res. A 2001, 460, pp. 138-145, doi: 10.1016/S0168-9002(00)01108-6.
23. Gmar, M.; Agelou, M.; Carrel F.; Schoepff, V. GAMPIX: a new generation of gamma camera. Nucl. Instrum. Methods Phys. Res. A 2011, 652, pp. 638-640, doi: 10.1016/j.nima.2010.09.003
24. Gottesman, S.R.; Fenimore, E.E. New family of Binary Arrays for Coded Aperture Imaging. Appl. Opt. 1989, 28, N° 20, pp. 4344- 4352.
25. Amoyal, G.; Schoepff, V.; Carrel, F.; Lourenco, V.; Lacour, D.; Branger, T. Metrological characterization of the GAMPIX gamma camera. Nucl. Instrum. Methods Phys. Res. A 2019, 944. p. 162568, doi: 10.1016/j.nima.2019.162568.
26. Carrel, F. et al. GAMPIX: A new gamma imaging system for radiological safety and Homeland Security Purposes. In Proceedings of 2011 IEEE Nuclear Science Symposium and Medical Imaging Conference (NSS/MIC), Spain, 23 October – 29 October, pp. 4739-4744, doi: 10.1109/NSSMIC.2011.6154706.
27. Amgarou, K.; Timi, T.; De Lanaute, N.B.; Carrel, F.; Schoepff, V.; Lemaire, H.; Gmar, M.; Abou Khalil, R.; Dogny, S.; Varet, T.; Patoz, A.; Talent, P.; Menaa, N. Evaluation of the next generation gamma imager. Conference record of 3rd International Conference on Advancements in Nuclear Instrumentation, Measurement Methods and Their Applications (ANIMMA) 2013, France, 23 June -27 June, pp. 1-6, doi: 10.1109/ANIMMA.2013.6728051.
28. Procz, S.; Lubke, J.; Zwerger, A.; Mix, M.; Fiederle, M. Optimization of Medipix-2 Threshold Masks for Spectroscopic X-Ray Imaging. IEEE Trans. Nucl. Sci. 2009, 56, pp. 1795-1799, doi: 10.1109/TNS.2012.2210909.
29. Turecek, D.; Holy, T.; Jakubek, J.; Pospisil, S.; Vykydal, Z. Pixelman: a multi-platform data acquisition and processing software package for Medipix2, Timepix and Medipix3 detectors. J. Instrum. 2011, 6 (C01046), p. C01046, doi: 10.1088/1748-0221/6/01/C01046
30. Czetina, A.; Hofstätter, M.; Schraml, S.; Hubner, M.; Sulzer, P.; Rothbacher, D.; Wurglitsch, R.; Riedl, E.; Sonntag, M.; Moser, S.; Fey, J. Robot assisted analysis of suspicious objects in public spaces using CBRN sensors in combination with high-resolution LIDAR*. In Proceedings of the 2019 IEEE International Symposium on Safety, Security, and Rescue Robotics (SSRR), Germany, 2 September - 4 September; pp. 256-262, doi: 10.1109/SSRR.2019.8848950.
31. Maier, D.; Blondel, C.; Delisle, C.; Limousin, O.; Martignac, J.; Meuris, A.; Visticot, F.; Daniel, G.; Bausson, P.; Gevin, O.; Amoyal, G.; Carrel, F.; Schoepff, V.; Mahe, C.; Soufflet, F.; Vassal, M. Second generation of portable gamma camera based on Caliste CdTe hybrid technology. Nucl. Instrum. Methods Phys. Res. A 2018, 912. pp. 338-342, doi: 10.1016/j.nima.2017.12.027.
32. Lee, W.; Wehe, D.K.; Jeong, M.; Barton, P.; Berry, J. A Dual Modality Gamma Camera Using LaCl3(Ce) Scintillator. IEEE Trans. Nucl. Sci. 2009, 56, pp. 308-315, doi: 10.1109/TNS.2008.2011051.
33. Lee, T.; Lee, W. Compact hybrid gamma camera with a coded aperturefor investigation of nuclear materials. Nucl. Instrum. Methods Phys. Res. A 2014, 767. pp. 5-13, doi: 10.1016/j.nima.2014.07.031.
34. Lee, T.; Kwak, S.; Lee, W. Investigation of nuclear material using a compact modified uniformly redundant array gamma camera. Nucl. Eng. Tech. 2018, 50, pp. 923-928, doi: 10.1016/j.net.2018.04.006
35. Turecek, D.; Jakubek, J.; Trojanova, E.; Sefc, L. Single layer Compton camera based on Timepix3 technology, J. Instrum. 2020, 15 (C01014), p. C01014.
36. Omata, A.; Kataoka, J.; Fujieda, K.; Sato, S.; Kuriyama, E.; Kato, H.; Toyoshima, A.; Teramoto, T.; Ooe, K.; Liu, Y.; Matsunaga, K.; Kamiya, T.; Watabe, T.; Shimosegawa, E.; Hatazawa, J. Performance demonstration of a hybrid Compton camera with an active pinhole for wide-band X-ray and gamma-ray imaging. Sci. Rep. 2020, 10, p. 14064, doi: /10.1038/s41598-020-71019-5.